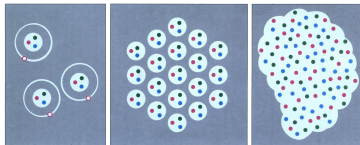


The Phase Diagram of Strong Coupling Lattice QCD including Gauge Corrections

Wolfgang Unger, Uni Frankfurt
with Philippe de Forcrand, Jens Langelage,
Kohtaroh Miura, Owe Philipsen

Lattice 2013, Mainz
1.08.2013

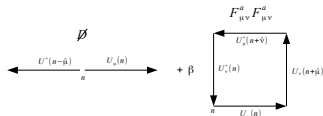


Why Strong Coupling Lattice QCD?

Look at Lattice QCD in a regime where the **sign problem** can be made **mild**:

$$\text{Strong Coupling Limit: } \beta = \frac{2N_c}{g^2} \rightarrow 0$$

- allows to integrate out the gauge fields completely, as **link integration factorizes**
 \Rightarrow no fermion determinant
- drawback: strong coupling limit is converse to asymptotic freedom, lattice is maximally coarse



Strong coupling LQCD shares important features with QCD:

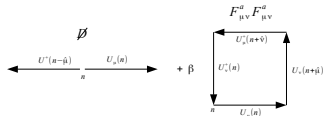
- exhibits **“confinement”**, only color singlet degrees of freedom survive:
 - mesons** (represented by monomers and dimers)
 - baryons** (represented by oriented self-avoiding loops)
- and **spontaneous chiral symmetry breaking/restoration**: (restored at T_c)
 \Rightarrow SC-LQCD is a great laboratory to study the full (μ, T) **phase diagram**

Why Strong Coupling Lattice QCD?

Look at Lattice QCD in a regime where the **sign problem** can be made **mild**:

$$\text{Strong Coupling Limit: } \beta = \frac{2N_c}{g^2} \rightarrow 0$$

- allows to integrate out the gauge fields completely, as **link integration factorizes**
 \Rightarrow no fermion determinant
- drawback: strong coupling limit is converse to asymptotic freedom, lattice is maximally coarse



Strong coupling LQCD shares important features with QCD:

- exhibits **“confinement”**, only color singlet degrees of freedom survive:
 - mesons** (represented by monomers and dimers)
 - baryons** (represented by oriented self-avoiding loops)
- and **spontaneous chiral symmetry breaking/restoration**: (restored at T_c)
 \Rightarrow SC-LQCD is a great laboratory to study the full (μ, T) **phase diagram**

SC-LQCD is a **1-parameter deformation of QCD in β**

Chiral transition and nuclear transition

This talk: focus on chiral transition and nuclear transition in the **chiral limit**

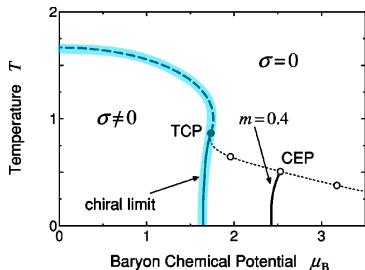
Chiral symmetry in SC-LQCD with **staggered fermions** for $N_f = 1$:

$$U(1)_V \times U(1)_{55} : \quad \psi(x) \mapsto e^{i\epsilon(x)\theta_A + i\theta_V} \psi(x), \quad \epsilon(x) = (-1)^{x_1+x_2+x_3+x_4}$$

- $U(1)_V$ baryon number conserved
- $U(1)_{55}$ chiral symmetry spontaneously broken at low temperatures/densities
- expected to be $O(2)$ 2nd order ($\mu = 0$)
- note: no chiral anomaly at $\beta = 0$

Nuclear Transition ($T=0$):

- baryon crystal forms
- chiral symmetry restored
- expected to be 1st order



Strong coupling phase diagram via
Mean field: Nishida, PRD 69 (2004)

Long History of Staggered SC-LQCD

Mean field ($1/d$ expansion):

1983: development of the technique [Kluberg-Stern, Morel, Petersson]

1985: first **finite density analysis** [Damgaard, Hochberg & Kawamoto]

1992: $T_c(\mu = 0) = 5/3$, $\mu_c(T = 0) = 0.66$ [Bilic *et al.*]

1995: entropy per baryon [Bilic & Cleymans]

2004: full phase diagram and location of (tri)**critical point** [Nishida]

2009: include $\mathcal{O}(\beta)$ corrections [Ohnishi *et al.*]

Monte Carlo:

1984: formulation as a **dimer system** [Rossi & Wolff]

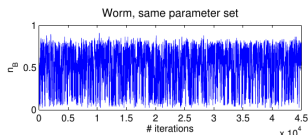
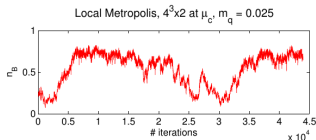
1989: first **finite density results** with MDP algorithm, $aT_c(\mu = 0) = 1.4$, $a\mu_c(T = 0) = 0.63$ [Karsch & Mütter]

2003: first **Worm algorithm** applied to U(3): **fast**, easy to do **chiral limit** [Adams & Chandrasekharan]

2010: full phase diagram and nuclear potential for SU(3) [de Forcrand & Fromm]

2011: continuous Euclidean time methods [de Forcrand & U.]

2011: include $\mathcal{O}(\beta)$ **corrections for U(3)** [Langelage, de Forcrand, Fromm, Miura, Philipsen, U.]



Strong Coupling Partition Function

After $SU(N_c)$ gauge link integration only **hadronic d.o.f.** survive:

$$M_x = \bar{\chi}\chi(x), \quad B_x = \frac{1}{N_c!} \epsilon_{i_1 \dots i_{N_c}} \chi_{i_1} \dots \chi_{i_{N_c}}$$

Exact rewriting after Grassmann integration: Mapping to a MDP representation:

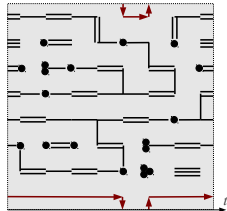
$$\mathcal{Z}(m_q, \mu, \gamma) = \sum_{\{k, n, \ell\}} \underbrace{\prod_{b=(x, \mu)} \frac{(N_c - k_b)!}{N_c! k_b!} \gamma^{2k_b \delta_{\mu 0}}}_{\text{meson hoppings } M_x M_y} \underbrace{\prod_x \frac{N_c!}{n_x!} (2am_q)^{n_x}}_{\text{chiral condensate } M_x} \underbrace{\prod_{\ell} w(\ell, \mu)}_{\text{baryon hoppings } \bar{B}_x B_y}$$

$$k_b \in \{0, \dots, N_c\}, \quad n_x \in \{0, \dots, N_c\}, \quad \ell_b \in \{0, \pm 1\}$$

- Grassmann constraint:

$$n_x + \sum_{\hat{\mu}=\pm\hat{0}, \dots, \pm\hat{d}} \left(k_{\hat{\mu}}(x) + \frac{N_c}{2} |\ell_{\hat{\mu}}(x)| \right) = N_c$$

- weight $w(\ell, \mu)$ and sign $\sigma(\ell) \in \{-1, +1\}$ for oriented baryon loop ℓ depends on loop geometry



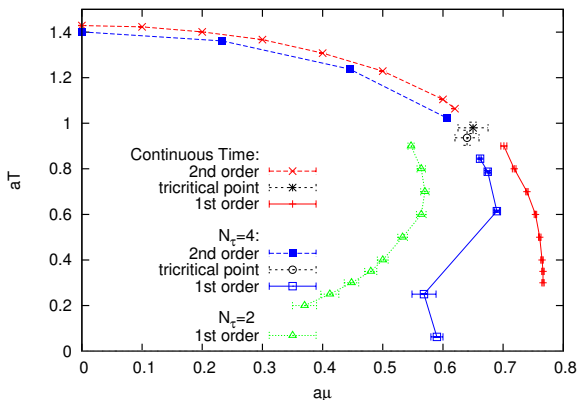
SC-LQCD Phase Diagram

Comparison of phase boundaries for $N_\tau = 2, 4$ and $N_\tau \rightarrow \infty$ (continuous time), studied with Worm algorithm [hep-lat/1111.1434]

identifications:

$$aT = \frac{\gamma^2}{N_\tau}$$

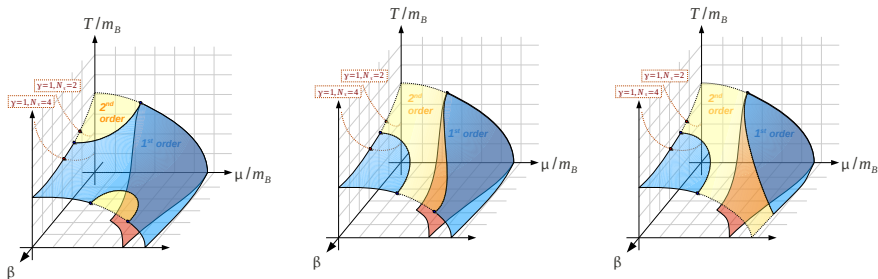
$$a\mu = \gamma^2 a_\tau \mu$$



- behavior at low μ qualitatively the same, first order transition shifts to larger μ
- no re-entrance in continuous time (also seen by [Ohnishi *et al.* 2012] via auxilliary field Monte Carlo, see also \rightarrow talk by T.Ichihara)

Connection Between Strong Coupling and Continuum Limit?

Various possible scenarios for the extension to finite β :



- back plane: strong coupling phase diagram
- front plane: continuum phase diagram ($N_f = 4$)

Questions we want to address:

- does **tricritical point** move to smaller or larger μ as β is increased?
- do the **nuclear and chiral transition split?**

Derivation of $\mathcal{O}(\beta)$ effective action

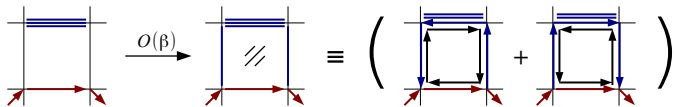
- Strong Coupling Partition function incorporating $\mathcal{O}(\beta)$ corrections:

$$Z = \int d\chi d\bar{\chi} dU e^{S_G + S_F} = \int d\chi d\bar{\chi} Z_F \langle e^{-S_G} \rangle_U$$

$$\langle O \rangle_U = \frac{1}{Z_F} \int dU O e^{-S_F}, \quad Z_F = \int dU e^{-S_F} = \prod_{l=(x,\mu)} z(x,\mu)$$

- plaquette expectation value before Grassmann integration:

$$\langle \text{tr}[U_P + U_P^\dagger] \rangle_U = \frac{1}{Z_F} \int dU \text{tr}[U_P + U_P^\dagger] e^{-S_F} = \left(\prod_{l \in P} z_l \right)^{-1} \sum_{s=1}^{19} F_P^s(M, B, \bar{B})$$



Link Integrations for $\mathcal{O}(\beta)$ diagrams

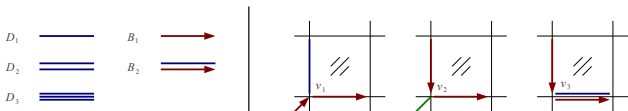
One-Link integrals for links on the edge of an elementary plaquette
(based on techniques from [Creutz 1978], [Azakov & Aliev 1988]):

$$\begin{aligned}
 J_{ik} = & \underbrace{\frac{1}{3} \bar{\chi}_k \varphi_i}_{D_1} - \underbrace{\frac{1}{6} M_\chi M_\varphi \bar{\chi}_k \varphi_i}_{D_2} + \underbrace{\frac{1}{12} M_\chi^2 M_\varphi^2 \bar{\chi}_k \varphi_i}_{D_3} + \underbrace{\frac{1}{12} \epsilon_{i_1 i_2} \epsilon_{kk_1 k_2} \bar{\varphi}_{i_1} \bar{\varphi}_{i_2} \chi_{k_1} \chi_{k_2}}_{B_1} \\
 & + \underbrace{\frac{1}{32} \epsilon_{i_1 i_2} \epsilon_{kk_1 k_2} M_\chi M_\varphi \bar{\varphi}_{i_1} \bar{\varphi}_{i_2} \chi_{k_1} \chi_{k_2} + \frac{7}{24} \bar{B}_\varphi B_\chi \bar{\chi}_k \varphi_i + \frac{1}{48} \epsilon_{i_1 i_2} M_\varphi B_\chi \bar{\varphi}_{i_1} \bar{\varphi}_{i_2} \bar{\chi}_k + \frac{1}{48} \epsilon_{kk_1 k_2} M_\chi \bar{B}_\varphi \chi_{k_1} \chi_{k_2} \varphi_i}_{B_2}
 \end{aligned}$$

- determine plaquette link product $P = \text{Tr} J_{ik} J_{kl} J_{lm} J_{mi}$
- result can be consistently re-expressed via

link weights: $w(D_k) = \frac{(N_c - k)!}{N_c! (k-1)!}$, $w(B_1) = \frac{1}{N_c! (N_c - 1)!}$, $w(B_2) = \frac{(N_c - 1)!}{N_c!}$

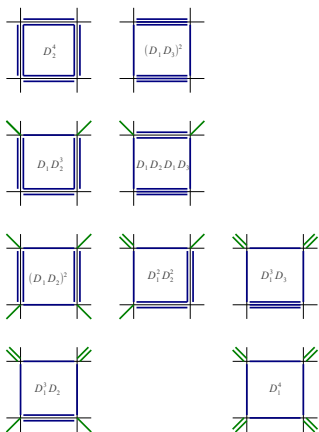
and **site weights:** $v_1 = N_c!$, $v_2 = (N_c - 1)!$, $v_3 = 1$



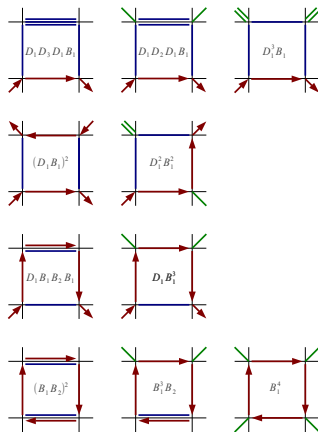
- Grassman constraint on sites touching a plaquette altered $N_c \rightarrow N_c + 1$

Classification of $\mathcal{O}(\beta)$ Diagrams

Diagrams classified by external legs (monomers or external dimers)



mesonic sector

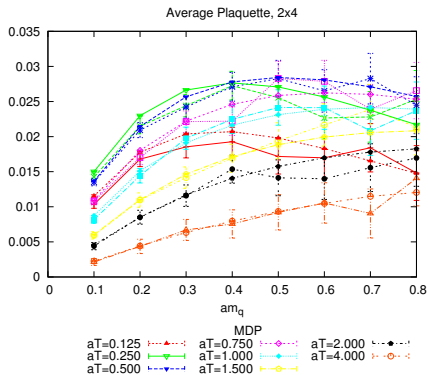
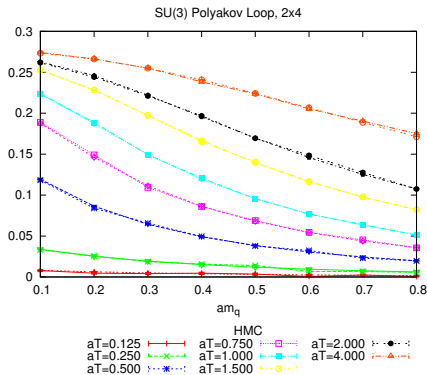


baryonic sector

Crosschecks at Finite Temperature

Croscheck on small lattices:

- comparison between **HMC** and **MDP** algorithms agrees well
- gauge observables are correctly obtained for **various** am_q , aT :

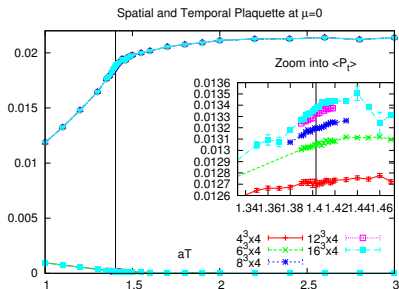
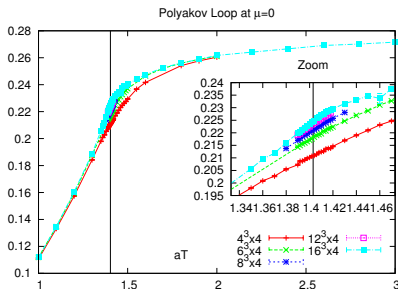


Gauge Observables at Zero Density

- Polyakov loop expectation value: ratio of partition function w/o static quark Q , measured via **reweighting from the SC-ensemble**:

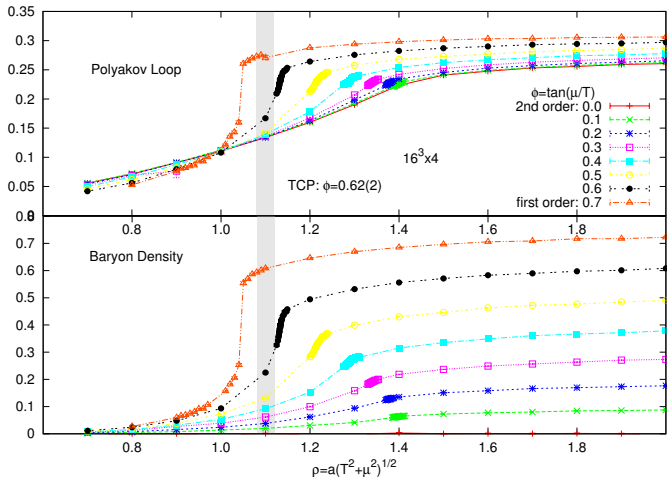
$$\langle L \rangle = \frac{\int d\bar{\chi} d\chi \langle L \rangle_U Z_F}{\int d\bar{\chi} d\chi Z_F} \sim e^{-(F_Q - F_0)/T} = \frac{Z_Q}{Z}, \quad L(\vec{x}) = \text{Tr} J_{N_\tau, 1}(\vec{x}) \prod_{t=1}^{N_\tau} J_{t, t+1}(\vec{x})$$

- $\langle L \rangle$ and $\langle P_t \rangle$ are sensitive to the chiral transition
- $\langle L \rangle$ rises significantly, indicating “deconfinement”



Gauge Observables at non-zero Density

- Scan at **finite density** in polar coordinates $(aT, a\mu) \mapsto (\rho, \phi)$
- Polyakov loop behaves similar to baryon number density, but also receives contributions from mesons



Chiral susceptibility in the chiral limit

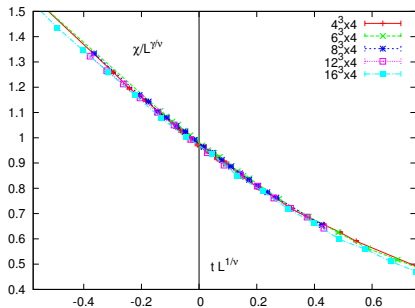
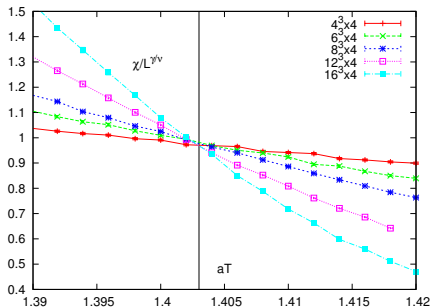
Full chiral susceptibility: $\chi = \frac{1}{V} \frac{\partial^2}{\partial (2am_q)^2} \log Z$ can be expressed in terms of monomers:

$$\chi = \frac{1}{(2am_q)^2 L^3 N_t} (\langle N_M^2 \rangle - \langle N_M \rangle^2 - \langle N_M \rangle) = \frac{1}{L^3 N_t} \left(\sum_{x_1, x_2} G(x_1, x_2) - \frac{\langle N_M \rangle^2}{(2am_q)^2} \right)$$

In chiral limit:

- $\chi \sim \langle (\bar{\psi}\psi)^2 \rangle$ is measured with high precision via Worm estimator $G(x_1, x_2)$
- χ has no peak, FSS via: $\chi_L / L^{\gamma/\nu}(t) = A + BtL^{1/\nu}$, $t = \frac{T - T_c}{T_c}$

with **3d O(2) critical exponents**



Taylor Expansion for the Susceptibility

For **fermionic observables**, the leading order β correction can be measured:

- obtain the slope of the transition temperature w.r.t. β from a Taylor coefficient:

$$\chi(\beta) = \chi_0 + \beta c_\chi^{(1)} + \mathcal{O}(\beta^2) \quad \text{with} \quad \chi_0 = \frac{Z_2}{Z},$$

$$c_\chi^{(1)} = \left. \frac{\partial}{\partial \beta} \frac{Z_2(\beta)}{Z(\beta)} \right|_{\beta=0} = \langle (\bar{\psi}\psi)^2 P \rangle - \langle (\bar{\psi}\psi)^2 \rangle \langle P \rangle$$

- Z_2 : 2-monomer sector sampled by $G(x_1, x_2)$ via Worm,
- necessary condition: $c_\chi^{(1)}$ needs to obey **finite size scaling** to modify aT_c
- one can show that in the thermodynamic limit:

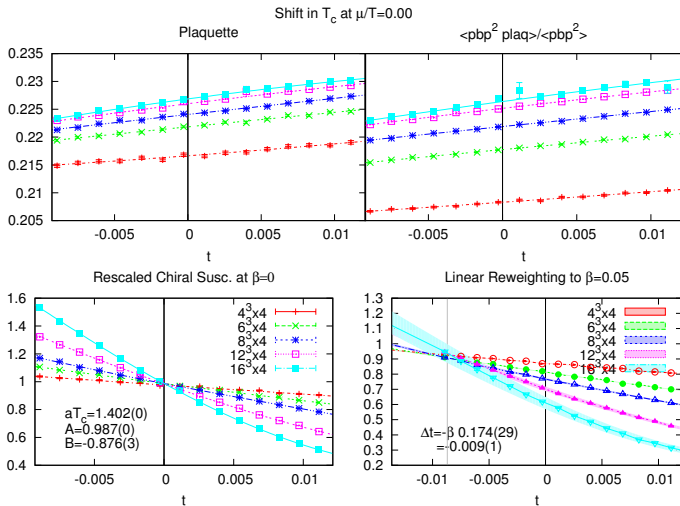
$$c_\chi^{(1)} \simeq (c_1 + c_2 L^{1/\nu} + c_3 t) \quad \text{in the vicinity of} \quad t = 0,$$

- the **shift in T_c** is then related to scaling function parameters A , B and c_2 :

$$\Delta a T_c(\beta) \doteq -\beta a T_c \frac{A}{B} c_2$$

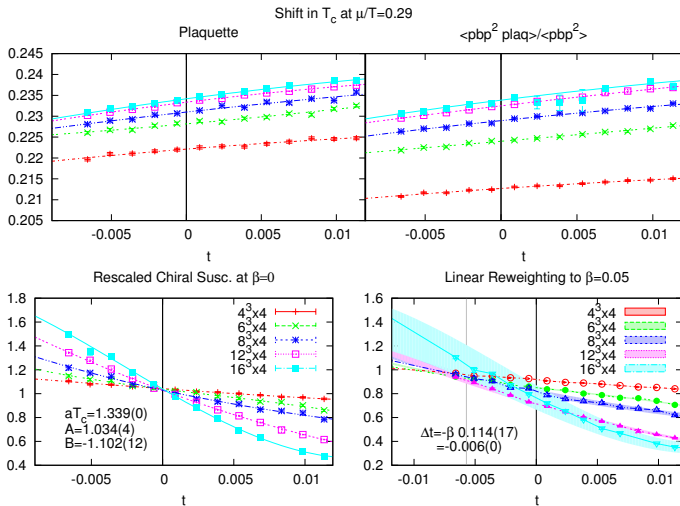
Results on the Slope at Zero and non-Zero Density

- We obtain for the **slope**: $\frac{\partial}{\partial \beta} aT_c(\beta) \simeq -0.24(3)$ at $\mu = 0$



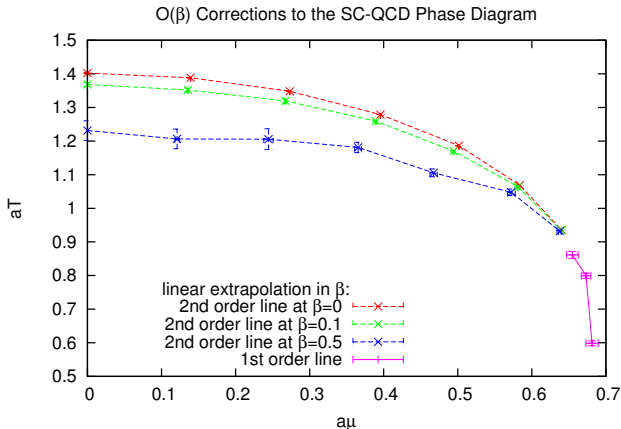
Results on the Slope at Zero and non-Zero Density

- We obtain for the **slope**: $\frac{\partial}{\partial \beta} aT_c(\beta) \simeq -0.15(2)$ at $\mu/T = 0.29$



Corrections to the SC-Phase diagram

- The slope vanishes at the tricritical point and along the first order line



ratio at strong coupling

$$\frac{T_c(\mu=0)}{\mu_c(T=0)} \approx \frac{1.403}{0.57} = 2.46$$

too large compared to $m_q = 0$ continuum result

$$\approx \frac{154 \text{ MeV}}{0.93 \text{ GeV}} = 0.165$$

but

$$\frac{T_c(\mu=0)}{\mu_c(T=0)} \searrow \quad (\beta \nearrow)$$

at leading $\mathcal{O}(\beta)$

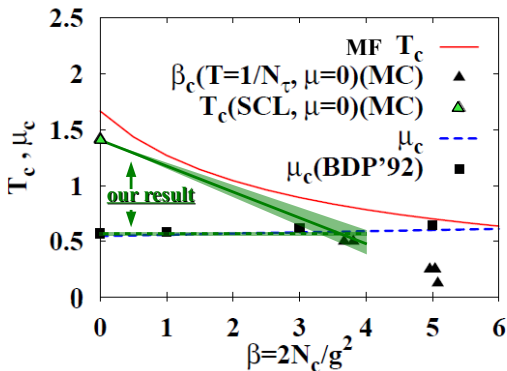
Conclusions

Achievements:

- correct average plaquette and Polyakov loop reproduced at $\beta = 0$ (checked with HMC)
- all measurements **extended to finite μ**
- $\langle L \rangle$ and $\langle P_t \rangle$ are sensitive to the chiral transition
- **slope of aT_c** determined at finite density up to the tricritical point

Further Goals:

- $\mathcal{O}(\beta^2)$ **corrections** needed
- determine whether the chiral and nuclear transition split at finite β



Comparison with mean field results by Miura *et. al*,
Phys. Rev. D **80** (2009) 074034 (2009): **good agreement**

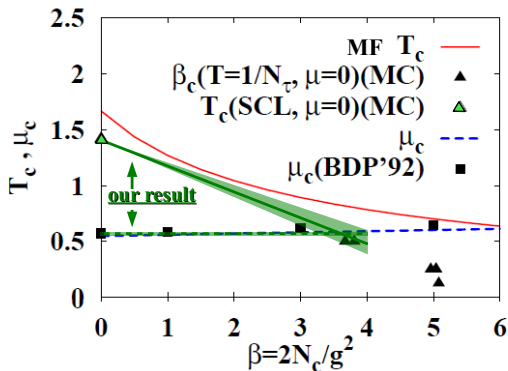
Conclusions

Achievements:

- correct average plaquette and Polyakov loop reproduced at $\beta = 0$ (checked with HMC)
- all measurements **extended to finite μ**
- $\langle L \rangle$ and $\langle P_t \rangle$ are sensitive to the chiral transition
- **slope of aT_c** determined at finite density up to the tricritical point

Further Goals:

- $\mathcal{O}(\beta^2)$ **corrections** needed
- determine whether the chiral and nuclear transition split at finite β



Comparison with mean field results by Miura *et. al*,
 Phys. Rev. D **80** (2009) 074034 (2009): **good agreement**

Thank you for your attention!

Backup: SC-LQCD at finite temperature

How to vary the temperature?

- $aT = 1/N_\tau$ is discrete with N_τ even
- $aT_c \simeq 1.5$, i.e. $N_\tau^c < 2 \Rightarrow$ we cannot address the phase transition!

Solution: introduce an **anisotropy** γ in the Dirac couplings:

$$\mathcal{Z}(m_q, \mu, \gamma, N_\tau) = \sum_{\{k, n, l\}} \prod_{b=(x, \mu)} \frac{(3 - k_b)!}{3!k_b!} \gamma^{2k_b \delta_{\mu 0}} \prod_x \frac{3!}{n_x!} (2am_q)^{n_x} \prod_l w(l, \mu)$$

Should we expect $a/a_\tau = \gamma$, as suggested at weak coupling?

- **No:** meanfield predicts $a/a_\tau = \gamma^2$, since $\gamma_c^2 = N_\tau \frac{(d-1)(N_c+1)(N_c+2)}{6(N_c+3)}$

\Rightarrow sensible, N_τ -independent definition of the temperature:

$$aT \simeq \frac{\gamma^2}{N_\tau}$$

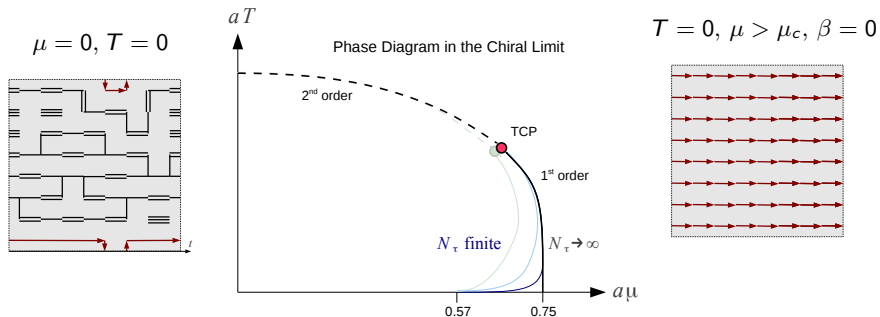
- Moreover, SC-LQCD partition function is a function of γ^2

However: **precise correspondence between a/a_τ and γ^2 not known**

Backup: The Fate of the Nuclear and Chiral Transition

Strong Coupling Limit:

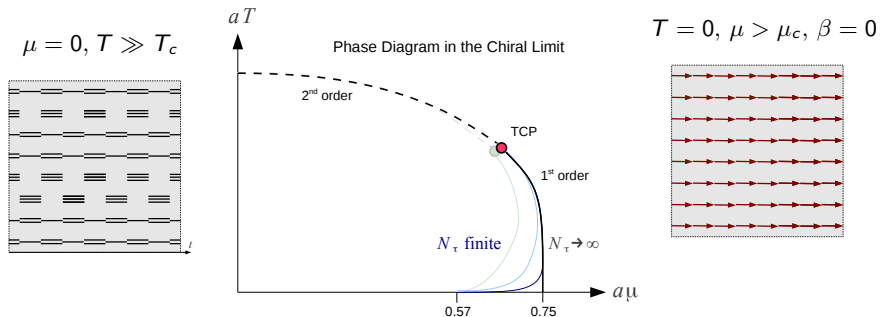
- finite temperature chiral transition takes place when spatial dimers vanish
- nuclear and chiral transition coincide: $\langle \bar{\chi}\chi \rangle$ vanishes as baryonic crystal forms



Backup: The Fate of the Nuclear and Chiral Transition

Strong Coupling Limit:

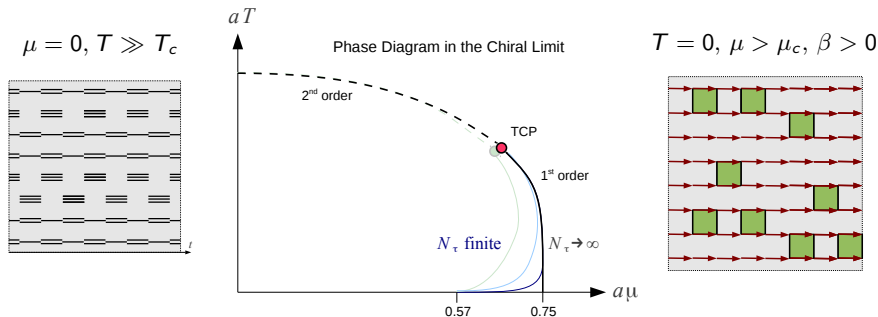
- finite temperature chiral transition takes place when spatial dimers vanish
- nuclear and chiral transition coincide: $\langle \bar{\chi}\chi \rangle$ vanishes as baryonic crystal forms



Backup: The Fate of the Nuclear and Chiral Transition

Strong Coupling Limit:

- finite temperature chiral transition takes place when spatial dimers vanish
- nuclear and chiral transition coincide: $\langle \bar{\chi}\chi \rangle$ vanishes as baryonic crystal forms



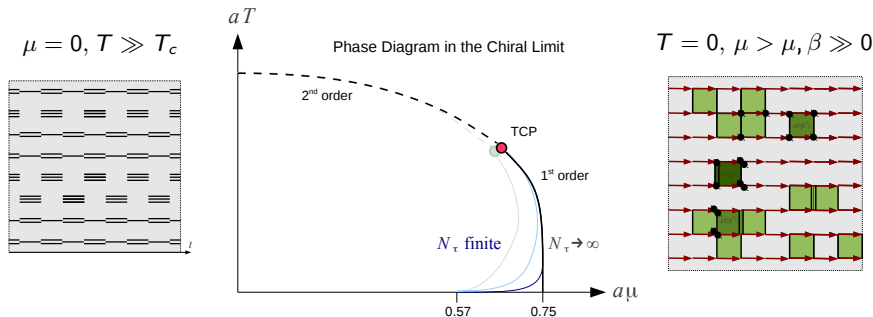
Possibility for $\beta > 0$:

- chiral transition takes place at larger μ_c than nuclear transition, as chiral condensate can be non-zero even though baryonic crystal has formed

Backup: The Fate of the Nuclear and Chiral Transition

Strong Coupling Limit:

- finite temperature chiral transition takes place when spatial dimers vanish
- nuclear and chiral transition coincide: $\langle \bar{\chi}\chi \rangle$ vanishes as baryonic crystal forms



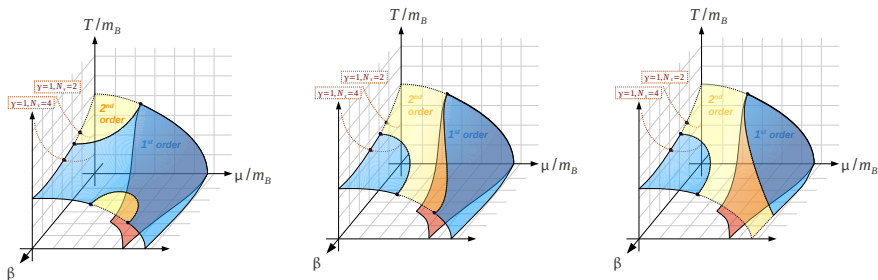
Possibility for $\beta > 0$:

- chiral transition takes place at larger μ_c than nuclear transition, as chiral condensate can be non-zero even though baryonic crystal has formed

Backup: The Fate of the Nuclear and Chiral Transition

Strong Coupling Limit:

- finite temperature chiral transition takes place when spatial dimers vanish
- nuclear and chiral transition coincide: $\langle \bar{\chi}\chi \rangle$ vanishes as baryonic crystal forms



Possibility for $\beta > 0$:

- chiral transition takes place at larger μ_c than nuclear transition, as chiral condensate can be non-zero even though baryonic crystal has formed

Backup Slide: SC + Plaquette Partition Function at $\mathcal{O}(\beta)$

partition function can be expanded up to $\mathcal{O}(1/g^{2N_c})$ as Grassmann integration terminates at this order:

$$Z = \int d\chi d\bar{\chi} Z_F \prod_P \left(1 + \frac{1}{g^2} \left(\prod_{l \in P} z_l \right)^{-1} \sum_{s=1}^{19} F_P^s + \dots \right)$$

- new set of **plaquette variables** $q_P \in \{0, \dots, N_c\}$ and auxiliary variables

$$q_x = \sum_P^{x \in P} q_P \in \{0, \dots, N_c\}, \quad q_b = \sum_P^{b \in P} q_P \in \{0, \dots, N_c\}$$

- help to write down Z after Grassmann integration:

$$Z = \sum_{\{k, n, \ell, q\}} \prod_{b=(x, \mu)} w_b \prod_x w_x \prod_\ell w_\ell \prod_P w_P,$$

$$w_x = \frac{N_c!}{n_x!} (2am_q)^{n_x} v_i(x), \quad w_b = \frac{(N_c - k_b)!}{N_c! (k_b - q_b)!}, \quad w_P = g^{-2q_P}$$

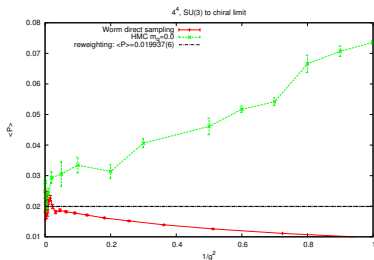
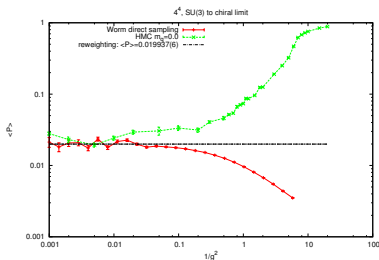
$$n_x + \sum_{\hat{\mu}=\pm\hat{0}, \dots, \pm\hat{d}} (k_{\hat{\mu}}(x) + \frac{N_c}{2} |\ell_{\hat{\mu}}(x)|) = N_c + q_x$$

Backup: Crosschecks at $\mu = 0, T = 0$

- Sampling average plaquette at finite β :

$$\langle P \rangle = \frac{2}{Vd(d-1)} \frac{\partial}{\partial \beta} \log(Z) = \frac{1}{\beta} \langle n_P \rangle, \quad n_P = \frac{2}{Vd(d-1)} \sum_P q_P$$

- **saturation expected:** $\langle n_P \rangle \leq \frac{N_c}{2d(d-1)}$
(at most N_c plaquettes can join at a bond or site)
- numerical results show indeed saturation of $\langle n_P \rangle$, $\Rightarrow \langle P \rangle \rightarrow 0$ for $\beta \rightarrow \infty$

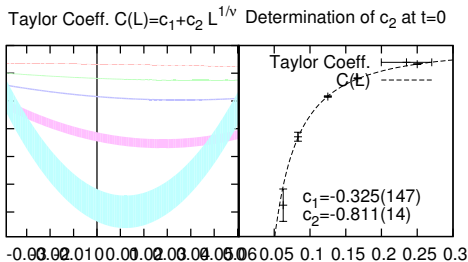
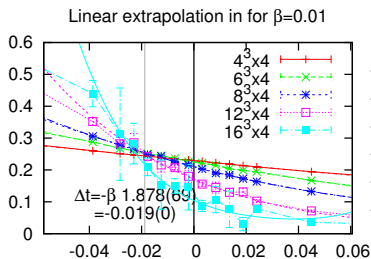
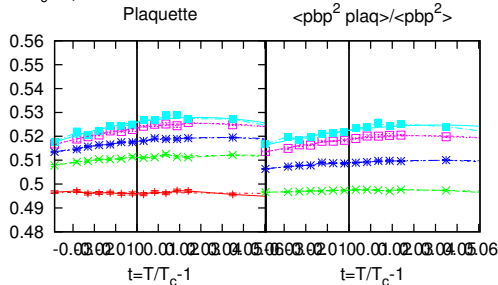
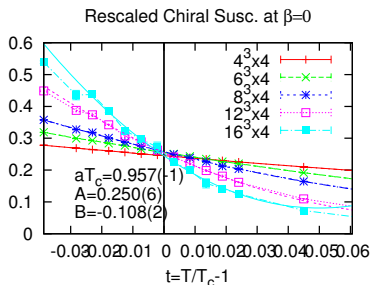


- reweighting from the SC-ensemble, $\langle P \rangle = Z_P/Z$, gives very precise results

Backup: FSS Scaling of Taylor Coefficient

Backup: FSS Scaling of Taylor Coefficient

Shift in T_c at $\mu/T=0.00$



Backup: Results on the Slope at Zero and non-Zero Density

The slope gets smaller for increasing μ

μ -dependence of the slope of the transition temperature

